**Article:**
Huescar Medina, C, Sattar, H, Phylaktou, HN et al. (2 more authors) (2015) Explosion reactivity characterisation of pulverised torrefied spruce wood. Journal of Loss Prevention in the Process Industries, 36. pp. 287-295. ISSN 0950-4230

https://doi.org/10.1016/j.jlp.2014.12.009

**TITLE: Explosion reactivity characterisation of pulverised torrefied spruce wood**

**AUTHORS:** Huéscar Medina* (**2 surnames**), Clara; Sattar, Hamed; Phylaktou, Herodotos N.; Andrews*, Gordon E.; Gibbs, Bernard M.

*Corresponding author E-mail: pm09chm@leeds.ac.uk and profgeandrews@hotmail.com

**AFFILIATION:** Energy Research Institute, School of Chemical and Process Engineering, University of Leeds, Leeds, LS2 9JT

## Abstract

Pulverised biomass is increasingly being used for power generation in 100% biomass plants or mixed with coal as a way of reducing greenhouse gas emissions. The fire and explosion hazards of pulverised wood and other agricultural waste materials have been recognised for some time. However, safety data for biomass are very scarce in the public literature, and non-existent for upgraded biomass products such as torrefied biomass. This is largely due to the challenges that biomass poses for explosion characterisation in the standard methods (1 $m^3$ ISO vessel or 20 L sphere). The authors have developed and calibrated a new system for the 1 $m^3$ ISO vessel that overcomes these challenges. In this work we present the first data in the open literature for the explosion characteristics of torrefied biomass. Results for untreated Norway spruce wood and Kellingley coal are also included for comparison. Flame speeds and post-explosion residue analysis results are also presented. Torrefied spruce wood was found to be more reactive than Kellingley coal and slightly more reactive than its parent material in terms of $K_{St}$, $P_{max}$ and flame speed. The differences between coal and biomass samples highlight that it should not be assumed that safety systems for coal can be applied to torrefied or raw wood materials without suitable modifications.

Keywords: dust explosion, biomass, torrefaction, reactivity, combustion

## 1. Introduction

Pulverised biomass (on its own or co-fired), accounted for nearly 14% of the total renewable electricity generation in the UK in 2012. The total contribution of renewable energy to all energy consumption in the UK was 3.8% in 2011. This comprised 8.7% of electricity, 2.2% of heat and 2.9% of transport fuel coming from renewable sources (DECC 2013). The UK has agreed to the EU wide renewable energy target of 20% of all energy to come from renewables by 2020, in line with the EU 2009 Renewable Energy Directive (European Parliament 2009). The UK's specific target is to achieve 15% of all energy from renewables. The UK's Department of Energy and Climate Change (DECC) has announced that the UK will attempt to meet this target with 30% renewable electricity, 12% renewable heat and 10% renewable transport fuel (Davey et al. 2011). As a result of the government’s plans, the use of biomass for generation of power, heat and transport fuels is forecasted to double or quadruple 2011’s levels by 2020 (from 12 TWh to 30-50 TWh) (Davey et al. 2011). Economic incentives are in place such as the renewable obligation certificates to achieve this. However, in power generation, there are challenges mainly related to retrofitting plants in order to use biomass, a material with different characteristics to fossil fuels that affect the general operation of plants: efficiency, storage, handling, etc.

Biomass properties can be upgraded through torrefaction. This is a thermal pre-treatment in which biomass is subjected to temperatures of around 300°C in an inert atmosphere for a certain period of time. The end product is more energy dense, hydrophobic and easy to grind with properties similar to low rank coals. Torrefaction of biomass decreases the transportation and storage costs and also enables co-milling with coal or for coal mills to be used with 100% torrefied biomass, which is attractive in the current scenario where authorities are encouraging

coal plants to co-fire or to convert to 100% biomass plants rather than building new 100% biomass plants.

The implicit assumption in replacing coal with biomass is that biomass behaves in a similar way to coal and therefore the present combustion and safety (fire and explosion) systems are adequate. The scarcity of explosibility data on biomass and the absence of any data for torrefied biomass prevent the informed assessment of suitability of the existing safety systems. The frequency of fire and explosion incidents in such plants (Butcher 2011; Holland 2011; Renewables International Magazine 2011) would suggest specific combustibility and explosibility data are required for biomass and treated biomass powders.

## 1.1 Biomass explosion characterisation challenges

Pulverised biomass and torrefied biomass present a few characteristics which pose challenges to the standard methods for determining explosion characteristics using the 1 $m^3$ ISO vessel or the 20 L sphere (British Standards Institution 2006). Wood biomass and some torrefied biomass materials can present very low bulk densities (ca. 200-300 $kgm^{-3}$), therefore the standard dust holders cannot hold enough dust for a complete characterisation of the samples. The addition of another 5 L volume dust holder used in parallel with the standard dust holder is required for low bulk density dusts in the standard, and this requires new calibration procedures if the same $K_{St}$ values are to be achieved. In addition, the fibrous nature of most biomass dusts prevents a correct dispersion of dust from the external dust holder into the explosion vessel, with the standard injection system blocking with biomass and no biomass flows into the explosion chamber.

The flammability and reactivity of biomass and other low bulk density and fibrous dusts has been the object of study of many researchers. Early studies exist on the explosibility of non-

traditional dusts using the Hartmann tube/bomb (Jacobson et al. 1961; Nagy et al. 1965; Eckhoff 1977), however this method of explosion characterisation was abandoned due to bad dust dispersion amongst other issues (Makris et al. 1989). Using the current explosion characterisation methods (1 $m^3$ or 20 L sphere vessels), (Bartknecht 1989) extended the dust holder volume and proposed a longer ignition delay for the new system, however, the most reactive mixtures were not comparable to the standard. (Marmo 2010) studied the explosibility of textile fibres with a 20 L sphere using the rebound nozzle, however, there was no reference to dispersion problems. (Wilén et al. 1999) worked with fibrous biomass samples, different dispersion systems were tested and calibrated to give the same $K_{St}$ values as the standard system, however, the reproducibility of other parameters was not proven. (Amyotte et al. 2012) investigated the explosion characteristics of fibrous wood and polyethylene dusts of different particle size. At high concentrations and larger particle size part of the dust was placed directly inside the 20 L sphere fitted with a rebound nozzle. This practice (also used by (Iarossi et al. 2012), with polyamide and polyester fibres) was likely to result in variability of dust dispersion patterns, and the results from Amyotte et al. showed that the maximum explosion pressure for wood samples was indeed variable. The variability in $K_{St}$ was unfortunately not shown but it was likely to be larger, as the rate of pressure rise is typically more sensitive to dissimilar dispersion patterns. (Garcia-Torrent et al. 1998; Conde Lazaro et al. 2000) used extended 25 L dust holders for high dust loadings for hyperbaric explosion tests with biomass. They modified the ignition delay and dispersion pressure and in turn concluded that the results obtained were not comparable to the standard system due to varied turbulence levels. (Dyduch et al. 2013) obtained promising results using statistical methods for the measurement of explosion parameters. These improved the accuracy of measured explosion characteristics and could allow measurements of $K_{St}$ and $P_{max}$ of difficult dusts.

A further challenge in the explosion characterisation standard methods (also not specific to biomass powders only) is that after each test, residual masses of dust are found in the dust holder and in the explosion chamber (Pilão et al. 2006; Sattar et al. 2012). The remaining dust in the external holder does not take part in the explosion and therefore it should be taken into account and the concentration that actually participated in the explosions should be used. Most researchers and testing labs do not report or account for the non-injected powder. A further problem is the practice of reporting dust concentrations as $gm^{-3}$ and not as equivalence ratio which is a much more informative parameter. Expressing concentrations as equivalence ratios shows that most reactive mixtures of dusts are extremely rich, as opposed to the most reactive mixtures of gases, always found for mixtures slightly richer than the stoichiometric mixture. In many cases the elemental analysis of the dust is not given so it is impossible to know the stoichiometric concentration. Consequently explosions safety parameters are rarely linked to fundamental combustion parameters, the most important of which is to know where the flame reaction zone is relative to stoichiometric. In spite of the importance of the explosion flame speed, from which the burning velocity can be calculated, no such measurements of reactivity are made for pulverised dust, which makes any modelling of dust explosion protection impossible. The current rate of pressure rise reactivity data is entirely empirical. Flame speed data and flame front equivalence ratios are determined in the present work as well as the conventional empirical parameters.

A great challenge is also posed by the dust found inside the vessel after the explosion, since it is often a mixture of partially burnt and unburnt particles. Therefore, it is unclear whether this dust participated in the main combustion reaction. Previous work was carried out by the authors to investigate this matter (Sattar et al. 2012), otherwise this issue has rarely been acknowledged in the literature and the focus was only to investigate the difference in particle morphology before and after an explosion (Hertzberg et al. 1982; Wilén et al. 1999; Pilão et

al. 2006). Furthermore, an accurate measurement of minimum explosion concentrations (MEC) is unlikely with the standard methods, since it is difficult to accurately know the concentration that took part in the combustion. Previous work by the authors addressed this issue and new techniques have been explored in order to provide an accurate measurement of MEC (Huéscar Medina et al. 2013).

### 1.2 Reactivity of biomass and torrefied biomass

The work published on biomass explosibility in the literature is inconsistent with respect to the reactivity of biomass relative to coal (Wilén et al. 1999). For torrefied biomass the reactivity of samples has been investigated through low heating rate techniques such as thermogravimetric analysis and subsequent derivation of devolatilisation kinetics. These results have shown that torrefied materials would present higher activation energies ($E_a$) which increased with torrefaction severity (higher temperature and longer residence times) (Darvell et al. 2010; Broström et al. 2012). Torrefaction decreases the moisture and volatile content and increases the ash content, thus, the loss of volatiles and the presence of more ash could reduce the reactivity of torrefied materials at the same time that less moisture content could increase it. Particle size could also affect the relative reactivity of torrefied biomass since torrefied biomass becomes more brittle with increased torrefaction severity and therefore when a raw biomass and a torrefied biomass are pulverised through the same procedure, torrefied material is bound to have a higher proportion of fines than the raw parent material. Previous work by the authors (Huéscar Medina et al. 2013) showed that MEC of torrefied samples occurred at lower equivalence ratios (Ø~0.2) than for coal (Ø~0.5) which indicates higher reactivity of torrefied materials in comparison to coal.

### 1.3 Objectives

The objective of this work is to present the first results available in the open literature for torrefied biomass using the standard 1 $m^3$ ISO vessel for the explosion characterisation of dusts. MEC, $K_{St}$ and $P_{max}/P_i$ have been measured and compared to its raw parent material and to coal explosibility data. Residues after explosions were collected and further analysed to understand its origin and to correct for the concentration that actually took part in the explosion, so that the flame front equivalence ratio could be determined.

## 2. Experiments

### 2.1 Materials

The materials used in this study were a sample of raw Norway spruce wood and the same sample torrefied at 260°C for 13 minutes (supplied by Sea2Sky Energy Corporation). Results from this lab for Kellingley coal are also presented for comparison. All biomass samples, initially supplied in chips, were milled in stages using a Retsch Cutting mill SM100 and a Retsch Rotor Beater Mill SR200 for the torrefied sample, the raw sample required further milling in a Retsch Ultra Centrifugal Grinding mill ZM100, in order to achieve a size distribution that would allow the samples to flow through the explosion vessel's dispersion system (<60 μm). All samples were stored in sealed containers.

Difficulties were generally encountered in sourcing materials in sufficient quantities to fully characterise their explosibility. In this particular case it was possible to source enough torrefied material; however, it was only possible to establish a trend for the characterisation of the raw sample for comparison.

After every test conducted in the 1 $m^3$ vessel, residues were found inside both the dust holder and the explosion chamber. These residues were collected and weighed in order to determine more accurately the concentration of dust which actually exploded. The concentrations were

generally expressed as equivalence ratios rather than as concentrations in grams of fuels per $m^3$ of air, to compare samples with different elemental compositions. The stoichiometric air to fuel ratio $(A/F)_{stoich}$ was calculated from the theoretical full combustion of the fuel in air based on the elemental analysis (see Table 1). The partially burnt residue inside the explosion chamber was collected and further analysed for elemental and proximate analysis, particle size distribution, morphology, and true density.

## 2.2 Fuel characterisation

All samples, before and after explosion, were analysed for its chemical composition through elemental and TGA-proximate analysis using, respectively, a Flash 2000 Thermo Scientific C/H/N/S analyser (O content was determined by subtraction), and a TGA-50 Shimadzu analyser using the temperature program used by (Biagini et al. 2006). The gross calorific value (GCV) of the samples was calculated from the elemental composition using the relation proposed for biomass in (Friedl et al. 2005).

The elemental composition in terms of C, H, O, N and S was used to calculate the stoichiometric fuel to air ratio (F/A) by balancing the combustion equation in air assuming the fuel formula is $CH_yO_zN_wS_k$ where y, z, w and k are the atomic ratios to carbon of hydrogen, oxygen, nitrogen and sulphur respectively.

$$CH_yO_zN_wS_k + aO_2 \rightarrow bCO_2 + cH_2O + dNO_2 + eSO_2$$

The stoichiometric fuel to air mass ratio is given by:

$$Stoichiometric\ \left({}^{F}/_{A}\right) = \frac{(12 + y + 16z + 14w + 32k)}{\left[\left(1 + \frac{y}{4}\right) - \frac{z}{2} + w + k\right] \cdot \frac{32}{0.232}}$$

The stoichiometric (F/A) ratio can be expressed as grams of fuel per cubic meter of air by multiplying the stoichiometric fuel to air mass ratio by the density of air (1200 $gm^{-3}$). Therefore, the equivalence ratio corresponding to each concentration of dust tested can be calculated as:

$$\emptyset = \frac{Actual\ \left({}^{F}/_{A}\right) concentration\ (gm^{-3})}{Stoichiometric\ \left({}^{F}/_{A}\right)\ (gm^{-3})}$$

The bulk density of the samples was determined using a 25 mL graduated cylinder, and a weighing balance. The volume of the graduated cylinder was filled with an increasing mass of sample. Measurements of weight and volume were taken and the bulk density was calculated as the average of 10 mass to volume ratios. In addition the true density was measured using the AccuPyc 1330 Pycnometer. The morphology of particles was investigated using Scanning Electron Microscopy, and the particle size distribution was determined using a Malvern Mastersizer 2000 instrument.

## 2.3 Dust explosion characterisation

The explosion characteristics of all samples were determined using an ISO 1 $m^3$ vessel (actual 1.138 $m^3$) (International Organization of Standardization 1985), modified and calibrated to handle fibrous biomass particles (Fig.1 (a)). The standard 5 L dust holder was extended to a larger 10 L volume suitable for containing larger quantities of low bulk density materials (such as biomass) and a calibration for this modified dust holder was developed (Sattar et al. 2013) to give the same results as for the standard system for cornflour. The initial mass of dust was placed inside the 10 L pot pressurised to 10 bars. Sattar et al. found that using an extended 10 L dust holder the turbulence levels at the time of ignition were different as those of the standard system. It was found that the mass of air delivered from the dust holder to the

explosion chamber was larger using the standard 20 bar pressurisation. However, when the pressurisation was reduced to 10 bar the mass of air delivered was comparable. This setting was further verified to give comparable results to the standard 5 L-20 bar setting using gases and dusts.

Furthermore, due to the fibrous nature of the samples, it was necessary to replace the standard dispersion C-ring system with a new dispersion system that allowed a better flow of dust inside the explosion chamber. A spherical wall mounted nozzle was designed and calibrated to give the same results as the standard C-ring system. The spherical nozzle, shown in Fig. 1 (c), is only perforated in the front half of the 110 mm diameter sphere, 9 holes of 8 mm diameter and 24 holes of 16 mm were drilled in triangular pitch.

In order to calibrate the new dispersion system, the turbulence factor β for the 1 $m^3$ vessel at 0.6 s ignition delay was determined by performing gas explosions in laminar and turbulent conditions to derive $K_G$ at said conditions. Mixtures of 10% methane gas in air were prepared inside the 1 $m^3$ vessel by partial pressures. Ignition was provided by a 16 J capacitance spark with a 0.5 m long electrode extended to the centre of the vessel. For turbulent gas explosions, air from the dust holder pressurised to the corresponding pressure (20 bars with 5 L dust holder, 10 bars with 10 L dust holder) was injected prior to ignition. Such turbulence was analogous to that induced due to dust dispersion. Therefore, using the following expression:

$$\beta = \frac{K_{G_{Turbulent}}}{K_{G_{Laminar}}}$$

The turbulent factor for this vessel was found to be 4.03. The requirement for any new dispersion system was to provide the same turbulent factor as the C-ring at the standard ignition delay (0.6 s). The spherical nozzle was found to give the same turbulence factor with

an ignition delay of 0.50 s with 10% Methane explosions as shown in Fig.2. This was then validated with cornflour dust/air mixtures showing comparable results for $K_{St}$, $P_{max}$ and flame speeds. This method was preferred rather than calibrating solely the $K_{St}$ value with a standard dust in order to ensure that all parameters, not only $K_{St}$, but maximum pressure, flame speeds, percentage of mass burnt were comparable to those obtained with the standard 1 $m^3$ vessel.

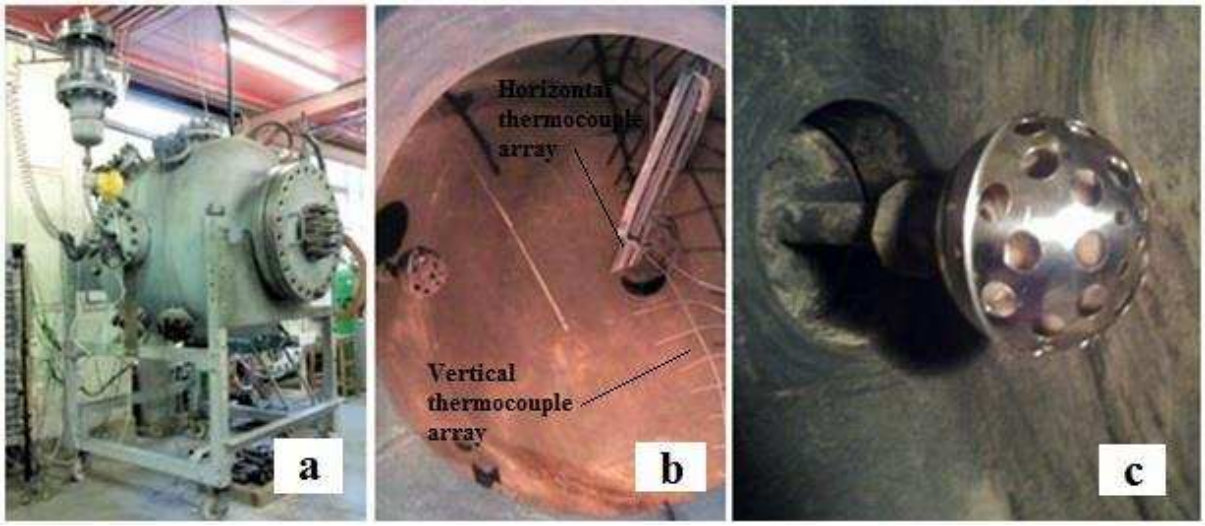


**Figure 1: (a) Leeds 1$m^3$ ISO vessel with 10 L dust pot, (b) Inner arrangement of the 1 $m^3$ vessel, (c) spherical disperser nozzle.**

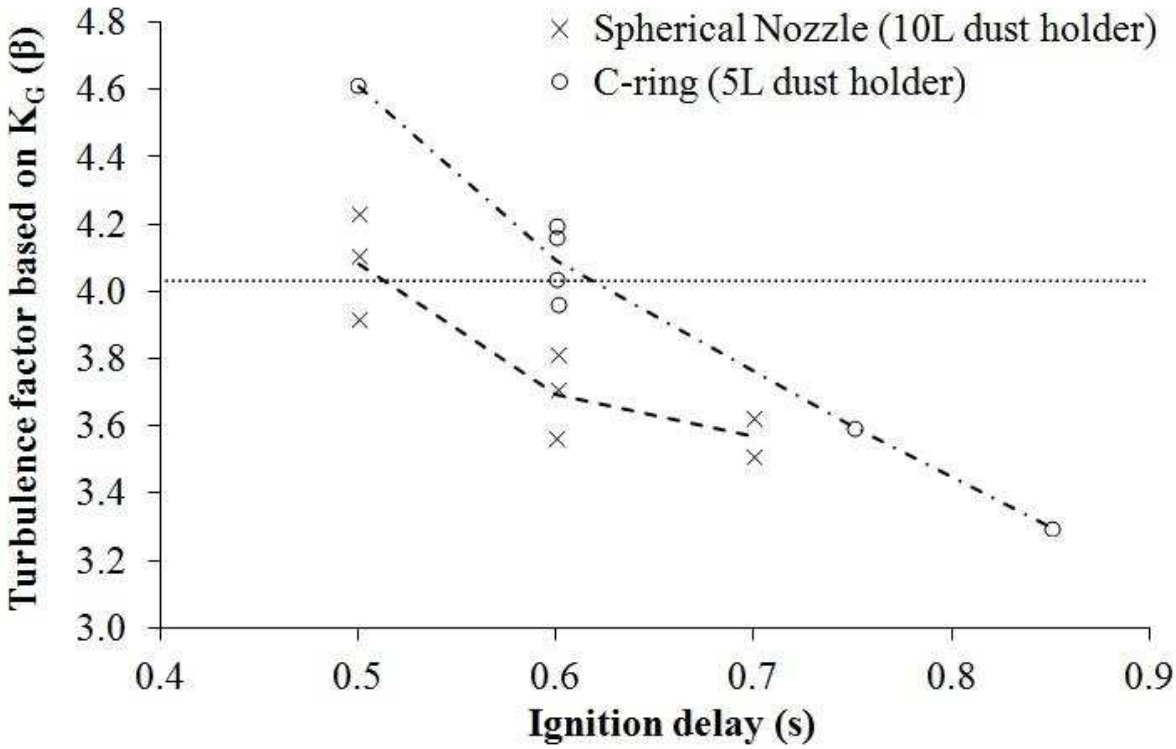


**Figure 2: Calibration of spherical nozzle**

The dust pressurised in the 10 L dust holder was released into the explosion chamber on activation of the electro-pneumatic valve on the interconnecting pipe. The dust cloud dispersed through the new spherical nozzle was ignited with two 5 KJ igniters placed in the centre of the explosion chamber after the recommended ignition delay for the spherical nozzle disperser of 0.5 s. The vessel was fitted with piezoresistive pressure transducers, which allowed the determination of maximum explosion pressures and rates of pressure rise, and arrays of type-K thermocouples in horizontal (left and right) and vertical (downward) directions (the arrangement is shown in Fig.(1.b)). These thermocouples were used to check that spherical flame propagation was achieved and to determine the time of flame arrival at each thermocouple position which allowed the derivation of flame speeds in all directions. The overall radial flame speed for a given test is the average of the flame speeds in each direction.

## 3. Results and discussion

### 3.1 Fuel characterisation

Table 1 shows the characterisation of all samples used. Some of the properties that differentiate biomass, torrefied biomass and coal can be observed; whilst the overall carbon content was similar at about 50% for all three fuels, there were significant differences in the fixed carbon content with raw biomass at 11% and 50% for coal. Torrefaction significantly increased the biomass fixed carbon content of the raw biomass by almost 50%. These differences suggest that most of the carbon in biomass is released as part of the volatile compounds as CO as there is insufficient hydrogen in biomass for the volatiles to be predominantly $CH_4$, as is commonly assumed.

Biomass had more than double the volatile content of coal, which reduced slightly when biomass was torrefied. The bulk density of biomass is less than half that of coal and the calorific value is about 35% lower. The energy density data calculated in Table 1 shows the biomass powder had less than 1/3 of the energy density of coal and although torrefaction increases the energy density of biomass by approximately 40% it is still less than half that of coal. These data suggest a significant impact on transport efficiency for the three fuels.

The oxygen and volatile content in raw biomass are more than double that of coal and they are only slightly reduced after torrefaction (the level of change after torrefaction would be dependent on the torrefaction conditions).

The particle size analysis data highlighted the difficulty in grinding untreated biomass samples. Despite being subjected to an additional grinding stage the raw biomass sample contained larger particles than the torrefied sample. Although all samples were milled to <60 μm, due to the fibrous nature of the biomass samples, thin but long particles could pass

through the sieve and therefore the size distribution shows that bigger particles are present. The cumulative size distribution of all samples is shown in Fig.(3):

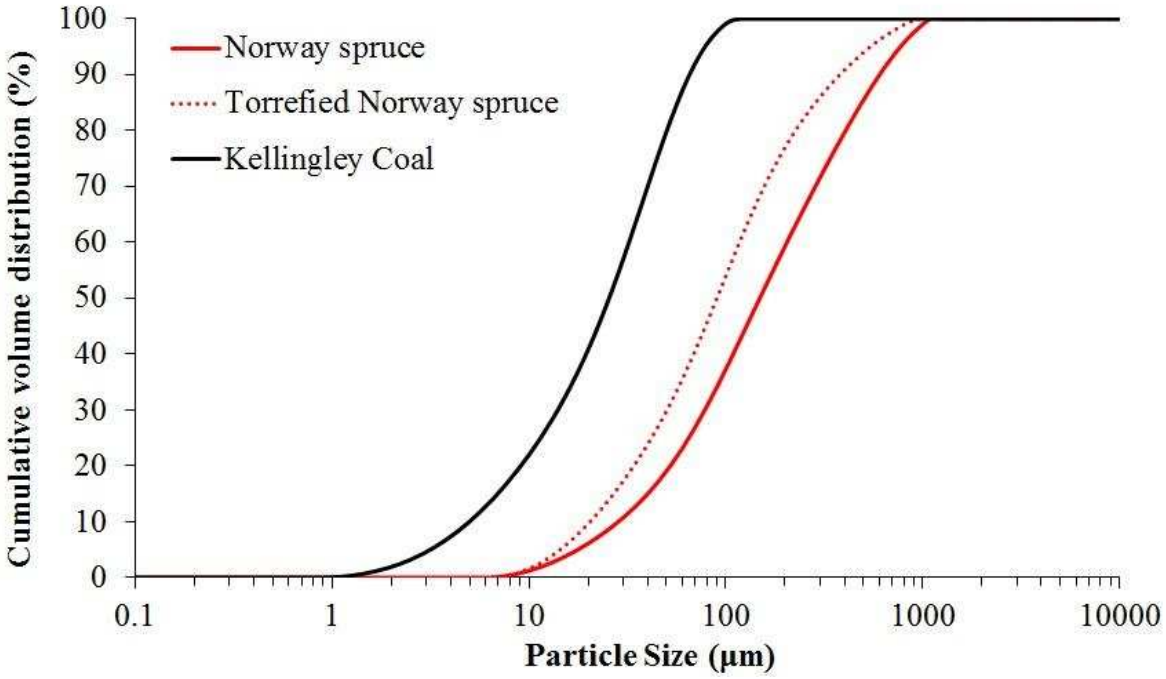


**Figure 3. Cumulative size distribution of raw and torrefied Norway spruce and Kellingley coal**

The stoichiometric fuel concentrations were different for each sample, and this was taken into account when comparing mixtures of fuel in air.

The standard (BSI 2004) requires keeping ¼ of the dust holder empty to achieve proper pressurisation, therefore the maximum quantity of torrefied spruce wood that could be tested in the 10 L external pot was to 1763 grams, which corresponds to a concentration of approximately 1500 $gm^{-3}$. For the raw wood sample no more than 1160 $gm^{-3}$ could be tested. It was also found that at high dust loadings (1250-1500 $g/m^3$) more than 10% of the initial mass was left in the dust holder after injection. Corrections for the undelivered dust were applied; therefore concentrations considered were injected concentrations.

**Table 1: Fuel characterisation**

| | Raw Norway Spruce | Torrefied Norway Spruce | Kellingley Coal |
|---|---|---|---|
| **Elemental analysis (% w/w)** | | | |
| **C** | 48.1 | 51.6 | 65.0 |
| **H** | 5.6 | 5.2 | 4.1 |
| **O** | 36.3 | 35.4 | 5.5 |
| **N** | 0.0 | 0.7 | 2.4 |
| **S** | 0.0 | 0.0 | 2.2 |
| **TGA-Proximate (% w/w)** | | | |
| **Moisture** | 5.8 | 2.8 | 1.7 |
| **Ash** | 4.1 | 4.2 | 19.1 |
| **Volatile Matter** | 79.0 | 77.0 | 29.2 |
| **Fixed Carbon** | 11.1 | 15.9 | 50.0 |
| **GCV ($MJkg^{-1}$)$_{daf}$** | 21.4 | 23.5 | 33.8 |
| **$(A/F)_{stoich}$** | 6.5 | 6.7 | 11.3 |
| **Stoich. fuel concentration ($gm^{-3}$)** | 184 | 178 | 106 |
| **Bulk Density ($kgm^{-3}$)** | 175.6 | 235.0 | 443.0 |
| **Energy density ($GJm^{-3}$)** | 3.8 | 5.5 | 14.9 |
| **Particle size distribution (µm)** | | | |
| **$D_{10}$** | 28 | 15 | 5 |
| **$D_{50}$** | 149 | 67 | 26 |
| **$D_{90}$** | 603 | 281 | 65 |

## 3.2 Explosion characteristics and flame speeds

Figure 4 shows the variation of $K_{St}$ and $P_{max}/P_i$ for different mixtures of dust and air. $K_{St}$ and the maximum pressure can be affected by a series of factors; $K_{St}$ is generally more affected by particle size or surface area, since it relates to how fast the combustion reaction occurs. On the

other hand, maximum pressures could be affected by factors that decrease the flame temperature such as the presence of moisture or ash. Volatile matter is also known to affect $K_{St}$ since devolatilisation will be faster when the size is small.

Coal particles were smaller than biomass or torrefied biomass samples but the volatile matter of the coal sample was also much lower. Overall, this particular coal sample had lower $K_{St}$. Also, a difference between coal and biomass is that $K_{St}$ for coal slowly decreases after the maximum value was reached for the most reactive concentration. However, for the torrefied sample, it was not possible to continue testing higher concentrations because the volume of dust exceeded ¾ of the dust pot volume and too much powder was left in the dust holder after the test. For this reason, to be able to assess $K_{St}$ for higher concentrations of dust it would be advisable to develop a delivery method in which the external dust injection was eliminated, by placing the dust inside the vessel and dispersing it from within. This is currently being developed by the authors using an injection method similar to that in the Hartmann explosion tube, where all the dust is placed inside the explosion vessel and then dispersed with a blast of air.

The parent material was tested at three concentrations around the most reactive mixture, showing similar values to the torrefied samples, only slightly lower. Also, the most reactive concentrations were found for concentrations much higher than stoichiometric for the biomass samples. The high $K_{St}$ values were found not to decrease much for richer mixtures, preventing the determination of a rich flammability limits. The literature on dust explosions shows that there are hardly any reported rich flammability limits and all data shows that the peak pressure remains high for all rich mixtures tested.

All the $K_{St}$ values are summarised in Table 2. Since all values are lower than 200 barms$^{-1}$, all the dusts tested are St-1 dusts (moderately explosible). With regard to maximum pressure, the

coal sample had lower maximum pressure probably due to the high ash content of the sample. Biomass samples, raw and torrefied, showed similar maximum pressures at around 9 bar.

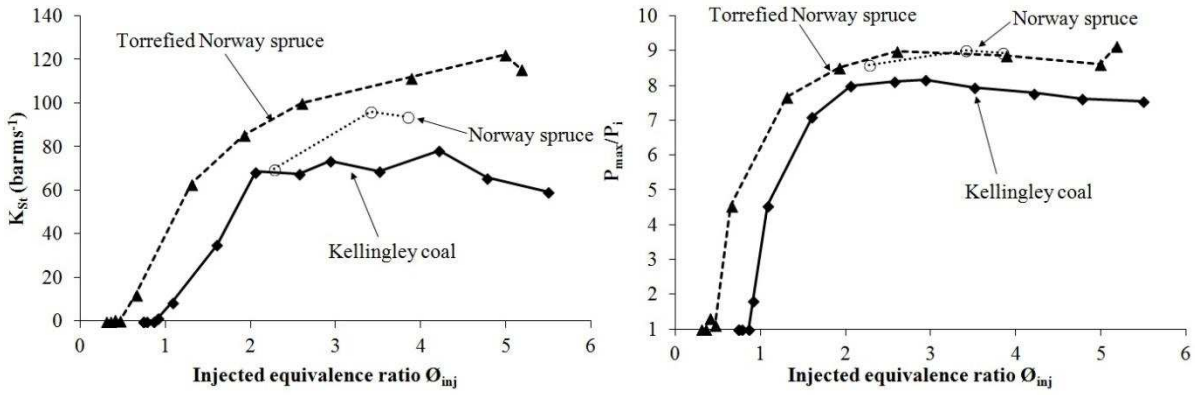


**Figure 4: $K_{St}$, $P_{max}/P_i$ for a range of Norway spruce wood, torrefied Norway spruce wood and Kellingley coal-air mixtures**

Figure 5 shows examples of the derivation of flame speeds in a test with raw Norway spruce wood and torrefied Norway spruce respectively. In each test three flame speeds were derived in horizontal right, left, and vertical downward directions. The distance from the spark of each thermocouple in the array is plotted against the actual time at which the flame reaches the thermocouple. A linear trend line can be fitted; the slope of such trend line is the average flame speed in each direction. The average flame speed for a test is the average of three flame speeds. It can be appreciated how the linear trends are parallel, which indicates spherical propagation.

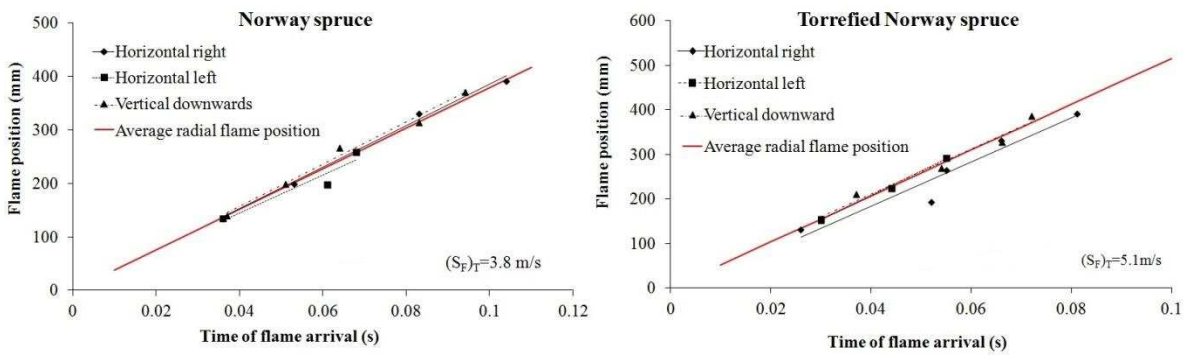

**Figure 5: Example of flame speed determination for a single test of Norway spruce and torrefied Norway spruce**

Figure 6 shows a linear relationship between $K_{St}$ and average flame speeds with correlation coefficients of 0.89, 0.95 and 0.96 for torrefied spruce wood, raw spruce wood and Kellingley coal respectively. The correlation between the two parameters suggests that either or both $K_{St}$ and flame speed could be used as measure of fuel reactivity.

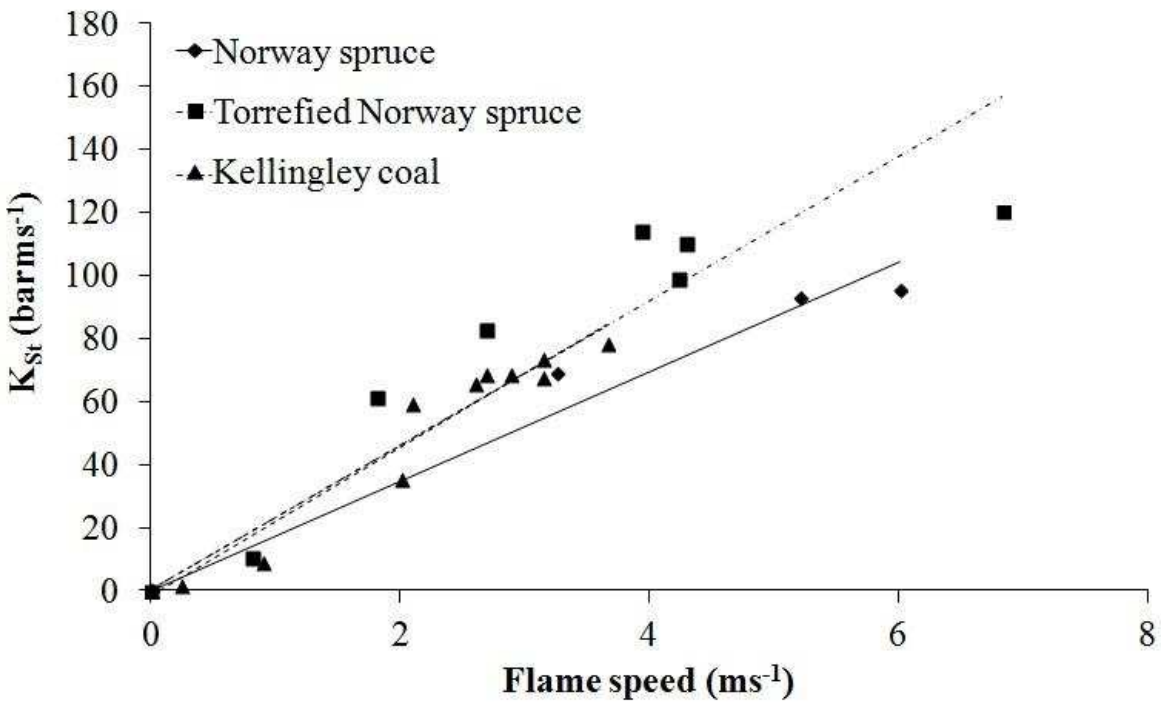


**Figure 6: Relationship of $K_{St}$ and flame speed**

**Table 2: Summary of explosion characteristics for Kellingley coal, Norway spruce wood and torrefied Norway spruce wood**

| **Sample** | **MEC ($gm^{-3}$)** | **$Ø_{MEC}$** | $K_{St}$ **($barms^{-1}$)** | **$P_{max}/P_i$** | **Flame Speed ($ms^{-1}$)** |
|---|---|---|---|---|---|
| **Kellingley Coal** | 91 | 0.86 | 78 | 8.2 | 3.6 |
| **Norway spruce wood** | - | - | 96 | 9.0 | 3.8 |

| | | | | | |
|---|---|---|---|---|---|
| **Torrefied Norway spruce wood** | 63 | 0.35 | 122 | 9.1 | 5.1 |

Table 2 summarises the explosion characteristics for the samples tested, which shows that torrefied spruce wood was the most reactive sample, with a minimum explosive concentration (MEC) of 62 $gm^{-3}$ which corresponds to an equivalence ratio of 0.35 and is lower than that of coal. However, it should be reminded that the calculation of the stoichiometry and hence the equivalence ratio is based on the elemental formula of the raw fuel and not of the volatiles that are actually burning.

## 3.3 Residue analysis

Dust residues were found inside the explosion chamber following explosion tests. These residues formed patched thin layers of material throughout the vessel walls. Particles closer to the walls appeared unchanged whilst particles in the upper part of the layer were clearly scorched by the flame front. Residues were collected using a conventional vacuum cleaner. In the process, residue samples were mixed thoroughly. The residues were then analysed in order to understand their origin and their role during explosion tests.

### 3.3.1 Elemental and proximate analysis

Table 3, presents the elemental composition for the samples before and after the explosion, as well as the proximate analysis and true density. The post-explosion samples analysed were the residues corresponding to the most reactive concentration. For the raw sample only 16% of volatiles were consumed, as opposed to 31% for the torrefied sample and 14% for the coal sample. This corroborated that the residues were not just remaining ash after combustion or ash plus char, with only volatiles burning. Previous work by the authors (Sattar et al. 2012; Sattar et al. 2012) with Kellingley coal explosion residues also showed an increase in fixed

carbon and ash. The trend was the same for Norway spruce and torrefied Norway spruce. Loss of volatiles and increase in ash and fixed carbon are characteristic of pyrolysis processes.

The residue's true density measurements showed an increase for Kellingley coal and torrefied wood between 6 and 10%, whereas the change was negligible in the case of raw wood. Therefore it is likely that the overall structure of coal and torrefied Norway spruce particles was changed, whereas unburned biomass particles remained largely unchanged.

**Table 3: Elemental, proximate and true densities before and after explosion**

| | **Pre-Explosion** | | | **Post-Explosion** | | |
|---|---|---|---|---|---|---|
| **Fuel Sample** | **Raw Norway Spruce** | **Torrefied Norway Spruce** | **Kellingley Coal** | **Raw Norway Spruce** | **Torrefied Norway Spruce** | **Kellingley Coal** |
| **Elemental analysis (% w/w)** | | | | | | |
| **C** | 48.1 | 51.6 | 65.0 | 48.4 | 55.4 | 64.3 |
| **H** | 5.6 | 5.2 | 4.1 | 5.4 | 4.1 | 3.5 |
| **O** | 36.3 | 35.5 | 5.5 | 26.6 | 27.1 | 7.1 |
| **N** | 0.0 | 0.7 | 2.4 | 0.0 | 1.4 | 1.4 |
| **S** | 0.0 | 0.0 | 2.2 | 0.0 | 0.0 | 2.2 |
| **TGA-Proximate (% w/w)** | | | | | | |
| **Moisture** | 5.8 | 2.7 | 1.7 | 3.1 | 3.6 | 1.6 |
| **Ash** | 4.1 | 4.3 | 19.1 | 16.6 | 8.5 | 19.9 |
| **Volatile Matter** | 79.3 | 77.0 | 29.2 | 66.5 | 53.4 | 25.0 |
| **Fixed Carbon** | 10.7 | 16.0 | 50.0 | 13.8 | 34.5 | 53.5 |
| **True Density ($kg/m^3$)** | 1546 | 1496 | 1484 | 1543 | 1591 | 1641 |

### 3.3.2 Particle size

The particle size distributions in Fig.7 show that for the raw biomass residue and original biomass sample had essentially the same size distribution. For torrefied biomass and coal, larger particles were present in the residue

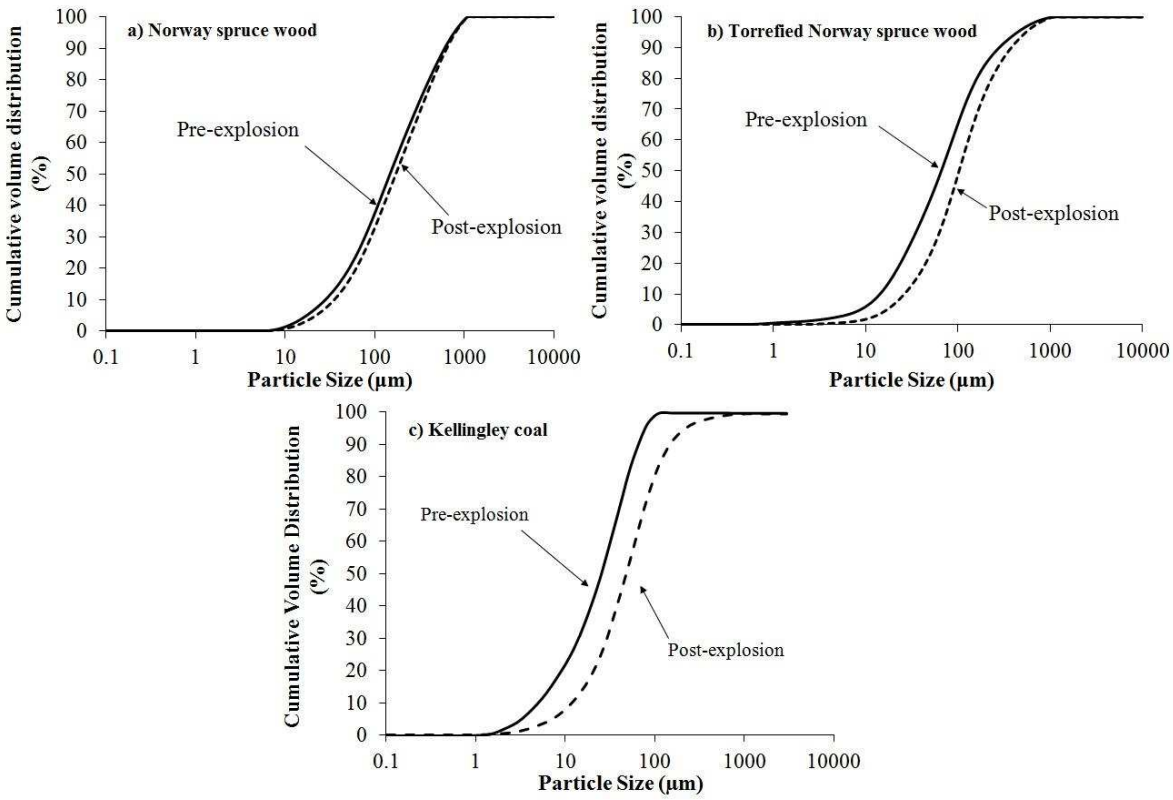


**Figure 7: Particle size cumulative distribution of Norway spruce wood, torrefied Norway spruce wood and Kellingley coal before and after explosion**

### 3.3.3 SEM

Figure 8 shows SEM images of the raw and torrefied wood samples prior to explosion (left) and of the residues corresponding to the most reactive mixtures (right). The original raw wood sample contained bigger particles than the torrefied sample before explosion, which confirms the particle size analysis results in Table 1 and Fig.(3) and highlights how torrefied wood samples are much easier to grind. Original torrefied wood particles had a fine needle shape, whereas the particles of raw wood resembled (comparatively) thick logs with irregular shapes.

The SEM images of torrefied biomass and coal residues show original particles mixed with some structurally different particles. These were char particles which are typically characterised by a round shape with blow out holes and by forming clusters with larger size (Cashdollar 2000). Therefore the reason for finding larger particles in the residues is due to the formation of these char structures rather than to selective burning of fine particles. These formations are rarely present in the raw wood residue, as reflected by the unchanged size distribution of the residue. For woody biomass it was found that the residue was virtually the same material as prior to the explosion, indicating that the particles burned during the explosion were fully consumed.

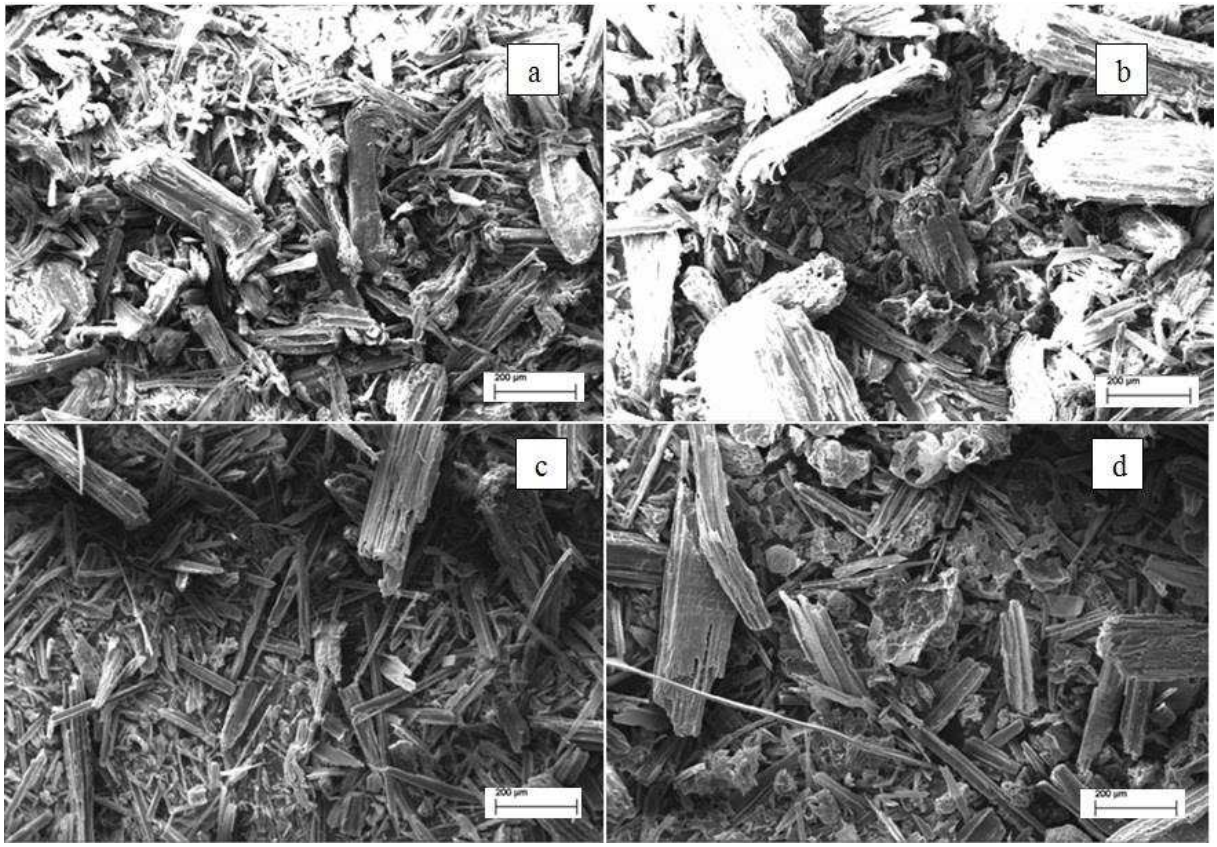


**Figure 8: SEM images at x200 magnification of (a) raw Norway spruce wood before explosion (b) raw Norway spruce wood after explosion of most reactive concentration.**

**(c) Torrefied Norway spruce wood before explosion. (d) Torrefied Norway spruce wood after explosion of the most reactive concentration**

The analysis of the residues suggest that these deposits could be a proportion of dust which was pushed by the explosion wind towards the walls, which formed a layer attached to the wall, compressed by the rising pressure. This layer would be pyrolysed by the impinging flame on the outer surface of the layer, but particles closer to the wall would remain unchanged. This would be consistent with visual observations when the vessel was opened following an explosion test. In the case of coal and torrefied biomass, char particles were formed by the action of the pyrolysing cooling flame in the wall whereas for biomass samples the formation of char seemed somehow inhibited.

It has been previously found in the literature that heating rates have a greater effect in the pyrolysis and formation of char of biomass than for coal. This behaviour has been attributed to the high cellulose content of biomass. At temperatures <300°C, cellulose dehydrates to a more stable anhydrocellulose which gives higher yields of char. However at high heating rates the residence time of biomass at <300°C is insignificant and therefore there is no time for dehydration of cellulose and formation of char (Zanzi et al. 1996). As torrefied biomass typically contains less cellulose than coal, since cellulose decomposes during the torrefaction treatment, more char particles were present in the pyrolysed residue in comparison to the residue of a raw biomass.

## 4. Conclusions

The explosion characteristics of Norway spruce wood torrefied at 260°C for 13 minutes have been measured in a 1 $m^3$ ISO vessel and compared to its parent material and a sample of Kellingley coal. The ISO 1 $m^3$ explosion vessel was modified, as allowed by the standard, by

increasing the dust holder volume to 10 L and replacing the standard C-ring for a spherical perforated nozzle mounted in the wall. The ignition delay was decreased to 0.5 s to achieve the same turbulence level as with the standard system. It was found that the new system is suitable for the characterisation of torrefied biomass pulverised under 60 μm. However, it would be possible to test higher concentrations of biomass if an in-vessel dispersion system was developed. Also samples with coarser particle size distributions could then be assessed for a more realistic approach to the actual particle sizes used in the industry.

Results have shown that torrefied Norway spruce presents chemical characteristics similar to low rank coals, grindability and calorific value are improved and volatile matter is decreased as well as moisture. Whilst the biomass energy density is significantly increased by torrefaction it remains less than half the energy density of coal.

MEC results for torrefied Norway spruce showed a similar behaviour to what has been typically found for other biomass samples, at equivalence ratios lower than typically found for coal. Kellingley coal was less reactive than torrefied Norway spruce wood, possibly due to its low volatile matter and high ash content. Turbulent flame speeds were measured in the explosions and showed a linear relationship with $K_{St}$, which indicates that flame speed can be used as a measure of reactivity as well as $K_{St}$. Flame speed is a more fundamental parameter that is more relevant in modelling of explosions. Both $K_{St}$ and flame speed measurements showed that torrefied Norway spruce was more reactive than the untreated biomass and Kellingley coal.

The analysis of the residue from an explosion test of torrefied Norway spruce presented loss of volatiles, increase in fixed carbon and ash contents, and presence of char structures. This behaviour is similar to that of coal, although the char yield appeared lower than for coal. In the case of raw biomass some oxygen had been released with the volatiles and also ash and

fixed carbon were increased. However, char particles were rarely present and the structure of the particles remained largely unchanged.

The analysis of all residues confirmed that a large proportion of the particles in the residue were unreacted and therefore it is believed that the loss of volatiles and increase in fixed carbon and ash was due to the action of the flame front acting on the residue as it cooled down in the vessel walls. The residue is formed by the explosion induced wind ahead of the flame entraining dust particles and pushing them towards the vessel walls. As the pressure raises these particles are compressed into a thin layer on the wall.

Char particles observed in coal and torrefied biomass explosion residues were almost non-existent in raw biomass residues. The amount of char produced could therefore be affected by the amount of cellulose in the original fuel and the high heating rates experienced by the particles in an explosion event. The formation of more char structures in torrefied biomass could be explained by the reduced cellulose content which is decomposed in the torrefaction pre-treatment itself. Further work is underway to corroborate and understand these findings using other torrefied and raw biomass materials and coal.

## Acknowledgements

The authors are grateful to the Energy Program (Grant EP/H048839/1) for financial support. The Energy Program is a Research Councils UK cross council initiative led by EPSRC and contributed to by ESRC, NERC, BBSRC and STFC.

## References

Amyotte, P. R., Cloney, C. T., et al. (2012). Dust explosion risk moderation for flocculent dusts. Journal of Loss Prevention in the Process Industries **25**(0): 862-869.

Bartknecht, W. (1989). Dust Explosions: Course, prevention, protection. London, Springer London.

Biagini, E., Barontini, F., et al. (2006). Devolatilization of Biomass Fuels and Biomass Components Studied by TG/FTIR Technique. Industrial & Engineering Chemistry Research **45**(13): 4486-4493.

British Standards Institution (2006). BS EN 14034-2: Determination of explosion characteristics of dust clouds Part 2: Determination of the maximum rate of explosion pressure rise of dust clouds. London, BSI. **BS EN 14034-2**.

Broström, M., Nordin, A., et al. (2012). Influence of torrefaction on the devolatilization and oxidation kinetics of wood. Journal of Analytical and Applied Pyrolysis **96**(0): 100-109.

BSI (2004). BS EN 14034-1: Determination of explosion characteristics of dust clouds Part 1: Determination of maximum pressure Pmax of dust clouds. London, BSI. **BS EN 14034-1**.

Butcher, J. (2011) Firefighters battle huge biomass fire at Port of Tyne. Last retreived from http://www.journallive.co.uk/north-east-news/todays-news/2011/10/31/firefighters-battle-huge-biomass-fire-at-port-of-tyne-61634-29689277/ on 31 October 2011

Cashdollar, K. L. (2000). Overview of Dust Explosibility Characteristics. Journal of Loss Prevention in the Process Industries **13**: 183-199.

Conde Lazaro, E. and Garcia Torrent, J. (2000). Experimental research on explosibility at high initial pressure of combustible dusts. Journal of Loss Prevention in the Process Industries **13**(0): 221-228.

Darvell, L. I., Jones, J. M., et al. (2010). Combustion properties of some power station biomass fuels. Fuel **89**(10): 90.

Davey, E., Jones, C., et al. (2011). UK Renewable Energy Roadmap. Department of Energy and Climate Change. London.

DECC (2013). UK Energy in Brief 2013.

Dyduch, Z. and Pekalski, A. (2013). Methods for more accurate determination of explosion severity parameters. Journal of Loss Prevention in the Process Industries **26**(6): 1002-1007.

Eckhoff, R. K. (1977). Pressure development during explosions in clouds of dusts from grain, feedstuffs and other natural organic materials. Fire Safety Journal **1**(2): 71-85.

European Parliament, C. o. t. E. U. (2009). Directive 2009/28/EC of the European Parliament and of the Council of 23 April 2009 on the promotion of the use of energy from renewable sources and amending and subsequently repealing Directives 2001/77/EC and 2003/30/EC (Text with EEA relevance)

Friedl, A., Padouvas, E., et al. (2005). Prediction of heating values of biomass fuel from elemental composition. Analytica Chimica Acta **544**(1-2): 191-198.

Garcia-Torrent, J., Conde-Lazaro, E., et al. (1998). Biomass dust explosibility at elevated initial pressures. Fuel **77**(9/10): 97.

Hertzberg, M., Cashdollar, K. L., et al. (1982). Domains of flammability and thermal ignitability for pulverized coals and other dusts: Particle size dependences and microscopic residue analyses. Symposium (International) on Combustion **19**(1): 1169-1180.

Holland, T. (2011) Essex fire destroys 21000 tonnes of woodchip destined for Dalkia biomass plant. Last retreived from http://www.mrw.co.uk/news/essex-fire-destroys-21000-tonnes-of-woodchip-destined-for-dalkia-biomass-plant/8617227.article. on 11 July 2011

Huéscar Medina, C., Phylaktou, H. N., et al. (2013). The development of an experimental method for the determination of the minimum explosible concentration of biomass powders. Biomass and Bioenergy **53**(0): 95-104.

Iarossi, I., Amyotte, P. R., et al. (2012). Explosibility of polyamide and polyester fibers. IX International Symposium on Hazards, Prevention and Mitigation of Industrial Explosions. Cracow, Poland.

International Organization of Standardization (1985). ISO-6184/1 Explosion Protection Systems- Part 1: Determination of Explosion Indices of Combustible Dusts in Air. Geneva. **ISO 6184-1:1985**.

Jacobson, M., Nagy, J., et al. (1961). Explosibility of agricultural dusts. Washington, D.C.**:** 23p.

Makris, A. and Lee, J. H. S. (1989). Lean flammability limits of dust-air mixtures. Archivum Combustionis **9**: 43-64.

Marmo, L. (2010). Case study of a nylon fibre explosion: An example of explosion risk in a textile plant. Journal of Loss Prevention in the Process Industries **23**(1): 106-111.

Nagy, J., Dorsett, H. G., et al. (1965). Explosibility of carbonaceous dusts. R.I. 6597. Washington, D.C.**:** 30 p.

Pilão, R., Ramalho, E., et al. (2006). Overall characterization of cork dust explosion. Journal of Hazardous Materials **133**(1-3): 183-195.

Renewables International Magazine (2011) Following explosion, world's largest pellet plant resumes operation. Last retreived from http://www.renewablesinternational.net/following-explosion-worlds-largest-pellet-plant-resumes-operation/150/515/31440/. on 15 July 2011

Sattar, H., Huescar Medina, C., et al. (2013). Calibration of a 10L volume dust holding pot for the 1m3 standard vessel, for use in low bulk density biomass explosibility testing. 7th International Seminar on Fire and Explosion Hazards, Providence, USA, Research publishing.

Sattar, H., Phylaktou, H. N., et al. (2012). Explosions and flame propagation in nut-shell biomass powders. IX International Symposium on Hazards, Prevention and Mitigation of Industrial Explosions. Cracow, Poland.

Sattar, H., Phylaktou, H. N., et al. (2012). Pulverised biomass explosions: Investigation of the ultra rich mixtures that give peak reactivity. IX International Symposium on Hazard, Prevention and Mitigation of Industrial Explosions. Cracow, Poland.

Wilén, C., Moilanen, A., et al. (1999). Safe handling of renewable fuels and fuel mixtures. Espoo, VTT Technical Research Cenre of Finland**:** 117 p.+app. 118p.

Zanzi, R., Sjöström, K., et al. (1996). Rapid high-temperature pyrolysis of biomass in a free-fall reactor. Fuel **75**(5): 545-550.